Cardiovascular Research (2013) **100**, 492–500
doi:10.1093/cvr/cvt215

Pericytes modulate endothelial sprouting

William G. Chang[1], Jillian W. Andrejecsk[2], Martin S. Kluger[3], W. Mark Saltzman[2], and Jordan S. Pober[4]*

[1]Department of Medicine and Section of Nephrology, Yale University School of Medicine, New Haven, CT 06520, USA, [2]Department of Biomedical Engineering, Yale University, New Haven, CT 06511, USA, [3]Department of Immunobiology, Yale University School of Medicine, New Haven, CT 06520, USA, and [4]Departments of Immunobiology, Pathology, and Dermatology, Yale University School of Medicine, 10 Amistad Street, Room 401D, New Haven, CT 06520, USA

Received 2 April 2013; revised 23 August 2013; accepted 11 September 2013; online publish-ahead-of-print 16 September 2013

Time for primary review: 37 days

Aim Angiogenic sprouts arise from microvessels formed by endothelial cells (ECs) invested by pericytes (PCs). The aim of this study was to examine the role of PCs in angiogenic sprouting, an understudied phenomenon.

Methods and results We adapted a human EC spheroid model to examine PC effects on vascular endothelial growth factor-A-induced EC sprouting *in vitro* by using Bcl-2-transduced human umbilical vein ECs to reduce apoptosis in collagen gels. Human placental PCs, separated from endothelial spheroids by a transwell, or addition of PC-conditioned media increased EC sprouting primarily through hepatocyte growth factor (HGF). Mixed endothelial–PC spheroids formed similar numbers of endothelial sprouts as endothelial spheroids but the sprouts from mixed spheroids were invested by PCs within 24 h. PCs were recruited to the sprouts by platelet-derived growth factor (PDGF)-BB; inhibition of PDGF signalling reduced PC coverage and increased EC sprouting. Transplanted endothelial spheroids give rise to sprouts *in vivo* that evolve into perfused microvessels. Mixed endothelial–PC spheroids form similar numbers of microvessels as endothelial-only spheroids, but acquire human PC investment and have reduced average lumen diameter.

Conclusions PCs promote endothelial sprouting by elaborating HGF, but when recruited to invest endothelial sprouts by PDGF-BB, limit the extent of sprouting *in vitro* and lumen diameter *in vivo*.

Keywords Endothelial cells • Pericytes • Bcl-2 • Platelet-derived growth factor • Hepatocyte growth factor

1. Introduction

Angiogenesis in adult vertebrates is initiated by endothelial cell (EC) sprouting from capillaries and post-capillary venules[1,2] in response to signals from hypoxic or injured tissues, such as vascular endothelial growth factors (VEGFs) or fibroblast growth factors, respectively.[3] These angiogenic proteins induce the ECs to invade the basement membrane and surrounding interstitium, forming columns of migrating cells known as 'sprouts'[4] that develop into new microvessels. The microvessels that give rise to sprouts are lined by ECs and are invested by contractile perivascular mural cells called pericytes (PCs).[5] PCs also appear to migrate outward from these microvessels and ultimately invest the newly formed sprouts, stabilizing sprouts as they mature into lumenized microvessels. Genetic or acquired deficiencies in PC coverage of EC-lined capillaries result in unstable microvessels.[6–8] While it is well established that PCs stabilize sprouting, it is unclear if they play a role in its initiation.

Sprouting can be modelled *in vitro* allowing more precise identification of signalling molecules. The best-described models of *in vitro* sprouting[9] include sprouting from aortic rings, collagen gel invasion by phorbol myristic acid-stimulated EC monolayers, and sprouting from EC spheroids (with or without bead support). The first two model systems are less amenable to studying human PCs; we therefore elected to adapt an EC spheroid model.[10,11] Because cultured ECs do not survive in three dimensional (3D) collagen gels much beyond 18–24 h,[12] we modified a previously described system to use human umbilical vein (HUV) ECs retrovirally transduced with anti-apoptotic protein Bcl-2 (Bcl-2-EC).[13–15] Bcl-2-EC spheroids retained the capacity to sprout in response to VEGF-A and cells forming the sprouts remain viable for several days. In this study, we used human placental PCs, the first readily abundant cultured source of this cell type, to examine the functions of PCs in spheroid sprouting. Here, we report that PCs stimulate sprouting largely through elaboration of hepatocyte growth factor (HGF) and then, after investing EC sprouts in response to platelet-

* Corresponding author. Tel: +1 203 737 2292; fax: +1 203 737 2293, Email: jordan.pober@yale.edu

derived growth factor (PDGF)-BB, stabilize and limit sprouting through contact-dependent signals.

2. Methods

2.1 Cells and reagents

HUVECs and human placental PCs were isolated from de-identified discarded tissues, and cultured as described previously[16,17] under protocols approved by the Yale Human Investigations Committee that conform to the principles of the Declaration of Helsinki. Such PCs uniformly express NG2, Thy-1, smooth muscle α-actin (SMA), calponin, CD146, and PDGFR-β, but lack smooth muscle cell (SMC) markers, SM myosin heavy chain and SM22-α, EC markers CD31 and CD34, and leucocyte markers CD45 and CD14.[16] Cells were used from passage level 1–5. To generate Bcl-2-ECs, HUVECs were retrovirally transduced with Bcl-2 as previously described.[15] VEGF-A (165 aa variant) was provided by the National Cancer Institute Biological Resources Branch Preclinical Repository (Rockville, MD, USA). VEGFR2 kinase inhibitor SU5416 (Sigma, St. Louis, MO, USA), recombinant HGF (R&D Systems, Minneapolis, MN, USA), and c-Met kinase inhibitor (Millipore Billerica, MA, USA, catalogue number 448101) were purchased.

2.2 Spheroid generation

Spheroids were generated by incubating suspended cells in 0.25% methylcellulose in Medium 199 (M199) supplemented with 20% foetal bovine serum in 96-well, non-adherent, *U*-bottomed plates (Fisher Scientific, Pittsburgh, PA, USA) as described.[10] Spheroids containing 2000 ECs were used for VEGF-A dose titration and transwell sprouting assays. Spheroids containing 500 ECs mixed with either 125 or 500 additional ECs or PCs were used in the mixed spheroid experiments. To distinguish the different cell types in mixed spheroids, ECs and PCs were labelled with PKH67 Green or PKH26 Red Fluorescent Cell Linker Kit (Sigma) per the manufacturer's recommendations prior to spheroid formation.

2.3 *In vitro* sprout measurements and imaging

To measure sprout lengths, images of the spheroids within the polymerized gels were captured using a Zeiss Axiovert 200M fluorescent microscope with a Hamamatsu ORCA-AG high-resolution camera and Volocity imaging software (PerkinElmer, Waltham, MA, USA). Sprout lengths were measured with National Institutes of Health (NIH) Image J. Cumulative sprout lengths (CSLs) for each condition were calculated by averaging the total sprout length of 10 individual spheres ± standard deviation (SD). Bcl-2-EC sprout coverage was calculated with NIH Image J from Leica TCS SP5 Spectral Confocal Microscopic images as a percentage of the total sprout length. Coverage of mural cells with Bcl-2-EC was verified with *Z*-stacks of sprouts with 5 μm slices and rotation of 3D projection.

2.4 *In vivo* implantation of spheroids and analysis of microvessel formation

All experimental protocols were approved by Yale's Institutional Animal Care and Use Committees (IACUC #2012-07863) and conform to the Guide for the Care and Use of Laboratory Animals. Collagen (1.5 mg/mL) gels (400 μL in volume) containing 250 spheroids with either 2000 ECs only or 2000 ECs with 500 PCs were polymerized in 48-well dishes and then implanted subcutaneously in the abdominal walls of 6–8-week-old female C.B-17 severe combined immunodeficiency/Bg mice, as described previously.[18] Gels were harvested 4 weeks after implantation. Vessel density was determined by dividing vessel number by gel area (mm^2) on haematoxylin and eosin (H&E)-stained mid-gel cuts. Lumen diameters of 100 vessels from three gels per group were analysed using NIH Image J.

2.5 Statistical analysis

Data are presented as means ± SDs. Non-linear regression modelling and best fit of VEGF-A dose–response was performed with an equilibrium binding model and statistically significant differences in CSL, sprout coverage, *in vivo* vessel density, and lumen diameters were determined by unpaired two-tailed *t*-tests with *post hoc* Bonferroni corrections for multiple comparisons as indicated. After verifying that our data sets were normally distributed by means of Anderson–Darling normality testing, the effects of titrations of different cell types were examined by two-way analysis of variance (ANOVA) with *post hoc* Bonferroni corrections (GraphPad PRISM software, La Jolla, CA, USA). This approach permits data to be pooled from independent experiments and allows the analysis of two independent categorical variables and the dependent variable.

3. Results

3.1 Analyses of paracrine effects of PCs on EC sprouting

We modified a cellular spheroid model to assess PC effects on sprouting angiogenesis *in vitro*. Consistent with the first report describing sprouting from spheroids,[11] EC spheroids in this modified system formed sprouts in response to VEGF-A in a dose-dependent manner (*Figure 1A* and *B*), quantified by measuring CSL as described in Section 2. Under these conditions, the level of sprouting plateaued at ~100 ng/mL of VEGF-A with a $K_d = 20.85$ ng/mL. Although HUVECs were uniformly viable within the spheroids at the time of transfer into collagen gels, most ECs were dead 24 h later by a live-/dead assay (*Figure 1C*). EC viability at this time point was only minimally improved by inclusion of VEGF-A in the collagen gels. We had previously shown that retroviral transduction of HUVECs to overexpress the anti-apoptotic protein Bcl-2 (designated as Bcl-2-ECs) permitted prolonged survival of individually suspended ECs within protein gels.[13] Therefore, we constructed spheroids using Bcl-2-ECs and observed that Bcl-2-EC sprouts remained nearly 100% viable at 24 h post-suspension in collagen (*Figure 1C*) and could be further maintained in collagen gels for at least 5 days. Interestingly, Bcl-2-EC spheroids sprouted without VEGF-A addition, although this basal response was small compared with that induced by VEGF-A. Importantly, like non-transduced ECs, Bcl-2-ECs sprouted in a VEGF-A dose-dependent manner (*Figure 1D* and *E*) with a $K_d =$ 1.85 ng/mL. HUVECs are not immortalized cells and multiple independent isolates had to be derived from multiple different donors to conduct these investigations. We observed variations in the absolute levels of sprouting from both non-transduced and Bcl-2-EC spheroids, likely due to donor variability, but all isolates tested showed qualitatively consistent patterns in response to the treatments described. Bcl-2-EC sprouts formed multiple contiguous cords of cells generally without lumens identifiable by light microscopy (*Figure 1F*). VEGF-A-induced sprouting of both non-transduced ECs and of Bcl-2-ECs could be blocked by the addition of VEGFR2 kinase inhibitor, SU5416, but basal sprouting of Bcl-2-ECs was not reduced (*Figure 1G*).

To examine paracrine effects of PCs on sprout formation, we polymerized collagen gels containing Bcl-2-EC spheroids within 0.4 μm pore size transwell inserts and suspended the inserts in media above cell monolayers formed from varying numbers of either human placental PCs or Bcl-2-ECs. While Bcl-2-EC monolayers had no effect on Bcl-2-EC sprouting from the spheroid in the upper compartment of the transwell, PC monolayers increased Bcl-2-EC sprouting in the absence and presence of VEGF-A in a cell number-dependent manner

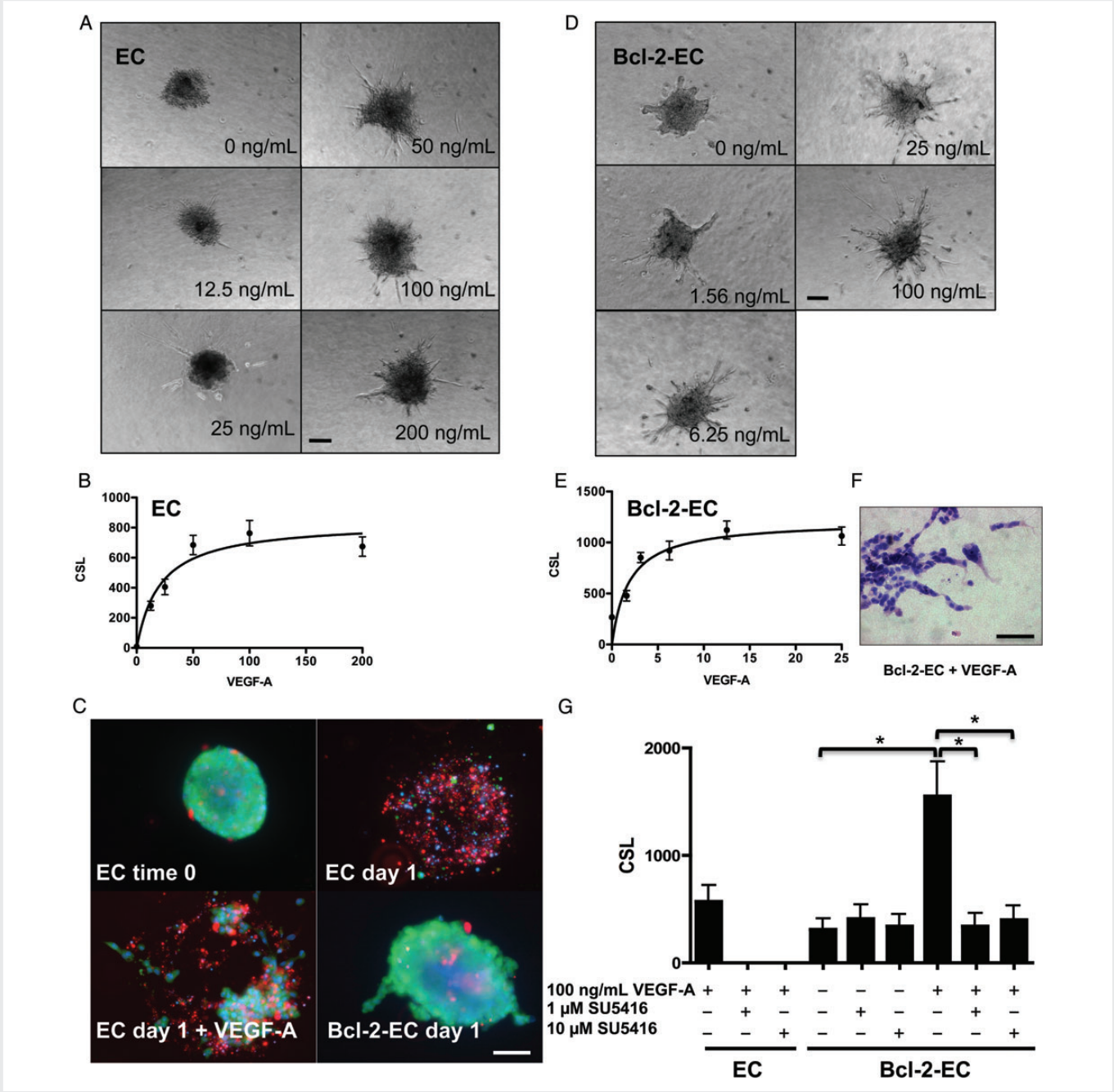

Figure 1 Sprout formation by EC and Bcl-2-EC spheroids in response to VEGF-A. (*A* and *D*) Phase contrast micrographs of (*A*) EC and (*D*) Bcl-2-EC spheroids embedded in collagen gels containing increasing concentrations of VEGF-A (ng/mL). (*B* and *E*) Non-linear regression modelling and best fit of (*B*) EC and (*E*) Bcl-2-EC CSL ± standard error as a function of VEGF-A concentration. (*C*) Live/dead cell survival assays with non-transduced ECs spheres at time 0, after 1 day ± 100 ng/mL VEGF-A in collagen gels or Bcl-2-EC spheroids after 1 day without VEGF-A. Live cells fluoresce (green), dead or damaged cell nuclei (red), and both live and dead nuclei (blue). (*F*) H&E of Bcl-2-EC spheroids after 1 day with 100 ng/mL VEGF-A. (*G*) The effect of VEGF inhibitor SU5416 on sprouting by EC and Bcl-2-EC spheroids. Scale bars are 100 μm (*A*, *D*, and *F*) and 60 μm (*C*). The asterisk indicates statistically significant difference by a two-tailed *t*-test with *post hoc* Bonferroni correction ($P < 0.017$).

(*Figure 2A* and *B*). Using two-way ANOVA with observations from multiple normalized experiments, we saw a statistically significant increase in sprouting with increasing PCs when compared with Bcl-2-EC monolayers (without VEGF-A, $N = 200$ individual spheroids from two independent experiments, $P < 0.0001$, and with VEGF-A, $n = 200$, $P < 0.0001$). Similar results were seen when non-transduced ECs were tested in this paracrine model (see Supplementary material online, *Figure S1*), although viability of ECs in the overlying spheroids and sprouts was limited to 24 h.

To determine whether PC-derived factor(s) that induce sprouting are stable, we prepared PC-conditioned media (CM) using the same culture conditions as employed in the transwell assays in the presence of VEGF-A and compared PC-CM with Bcl-2-EC-CM. We observed that PC-CM, but not Bcl-2-EC-CM, could stimulate Bcl-2-EC sprouting

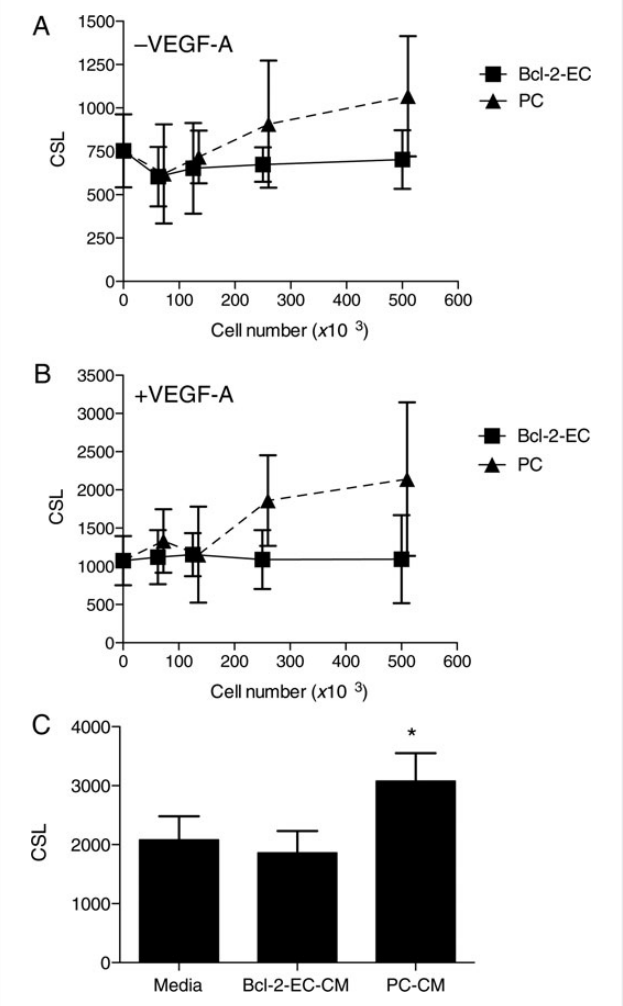

Figure 2 Effects of Bcl-2-ECs, PCs, and CM on Bcl-2-EC sprouting from spheroids. For the *in vitro* paracrine model (*A* and *B*), measurements shown of CSL ± SD from Bcl-2-EC spheroids in collagen gels cultured in transwells above monolayers of Bcl-2-ECs or PCs for 24 h in the absence (*A*) or presence (*B*) of 100 ng/mL VEGF-A. The x-axis indicates the number of cells in the monolayer times 10^3. CM or control (non-conditioned) medium was used to prepare collagen gels containing 100 ng/mL VEGF-A into which Bcl-2-EC spheroids were embedded and CSL was measured. (*C*) CSL in the presence of non-conditioned and CM from 5×10^5 Bcl-2-ECs and 5×10^5 PCs. The asterisk indicates a statistically significant difference by a two-tailed *t*-test.

(*Figure 2C*). Since Bcl-2-EC spheroids were cultured under conditions of maximal VEGF-A stimulation, it seems unlikely that additional paracrine stimulatory effects can be explained by PC production of VEGF-A. Similar results were obtained when PC-CM was tested against non-transduced ECs (data not shown).

We recently reported a gene expression microarray analysis of human placental PCs in monolayer culture.[16] These data revealed that human placental PCs express high levels of HGF mRNA, which is known to be pro-angiogenic.[19,20] We confirmed that human placental PCs secrete high HGF protein levels by enzyme-linked immunosorbent assay (ELISA), detecting a mean of 4.2 ± 3.5 ng/mL of HGF from five independent samples of PC-CM from 5×10^5 PCs after 24 h in 1 mL of M199 with 1% serum; no HGF was detected in the culture medium prior to conditioning nor in Bcl-2-EC-CM. Recombinant HGF stimulated sprouting by Bcl-2-EC spheroids both with and without added VEGF-A (*Figure 3A*). More importantly, complete immunodepletion of HGF from PC-CM, confirmed by ELISA, showed a 62.6 ± 14.9% reduction (from three independent experiments) of the stimulatory effect of PC-CM on EC sprouting (*Figure 3B*). The stimulatory effect of recombinant HGF was effectively inhibited by a c-Met receptor tyrosine kinase inhibitor (*Figure 3C*), and the stimulatory effect of PC-CM was partially blocked by the same inhibitor (*Figure 3D*). Thus, HGF appeared to be the major sprout-promoting factor produced by PCs.

3.2 Analyses of contact-dependent effects of PCs on angiogenesis

Our transwell and PC-CM experiments examined paracrine PC effects on EC sprouting *in vitro*. *In vivo*, sprouting arises from vessels in which ECs and PCs are in close contact and ends when PCs invest newly formed sprouts. To examine interactions between PCs and ECs under conditions that permit cell contact, we generated Bcl-2-EC/PC mixed spheroids by adding PCs to the Bcl-2-EC suspension during spheroid formation. As comparators, we added additional Bcl-2-ECs instead of PCs. The added cells were distinguished from the test Bcl-2-ECs by fluorescent membrane labelling (using PKH67 green for Bcl-2-ECs and PKH26 Red for added Bcl-2-ECs and PCs) prior to spheroid formation. Confocal fluorescence microscopic analyses with *Z*-series were taken to examine organization of the mixed spheroids. ECs and PCs organized into a PC core with a Bcl-2-EC outer layer, whereas green Bcl-2-EC/red Bcl-2-EC mixed spheroids were randomly intermixed (*Figure 4A*). In spheroids formed wholly from ECs labelled with different coloured fluorophores, EC incorporation into sprouts was random. In Bcl-2-EC/PC mixed spheroids, PCs migrated out of the spheroid and clearly invested the EC sprouts (*Figure 4B*). After 24 h, neither PCs nor additional Bcl-2-ECs significantly enhanced or reduced sprout formation by Bcl-2-EC spheroids (*Figure 4D* and *E*) when tested by two-way ANOVA (without VEGF-A, $n = 120$ and with VEGF-A, $n = 120$ individual spheroids from two independent experiments). However, when we examined mixed spheroids over several days, the presence of PCs significantly reduced both CSL and sprout number in the presence of VEGF-A by Day 2 (*Figure 4F* and *G*) when tested by two-way ANOVA ($n = 60$ spheroids from one experiment (*F*) $P < 0.0001$ and (*G*) $P < 0.017$ for all Bcl-2-EC compared with mixed spheroid groups). To further examine the temporal association of Bcl-2-EC sprouts and PCs, we carried out time-lapse observations of sprouting by mixed EC/PC spheroids (see Supplementary material online, *Videos S1* and *S2*). These demonstrate that Bcl-2-ECs over the first 8 h sprout independently of PCs but over a subsequent interval from 9 to 19 h, PCs are recruited to and invest Bcl-2-EC sprouts. By 24 h essentially all EC sprouts are invested by PCs and further increases in CSL cease. Thus, EC/PC mixed spheroids differ in this regard from EC-only spheroids, which continue to increase both the CSL and number of sprouts for an additional 24 h (*Figure 4F* and *G*). At these later times, transmission electron microscopy (TEM) using iron-labelled PCs show close contact of PCs and Bcl-2-ECs in the sprouts within the collagen gels (*Figure 4C*). TEM also detects the presence of small lumens within at least some of the EC sprouts that were not apparent by light microscopy.

It has been observed that both PDGF-B and PDGFR-β KO mice display deficiencies of PC coverage in developing vessels, resulting in microvascular leakage and haemorrhage.[21–23] To assess whether

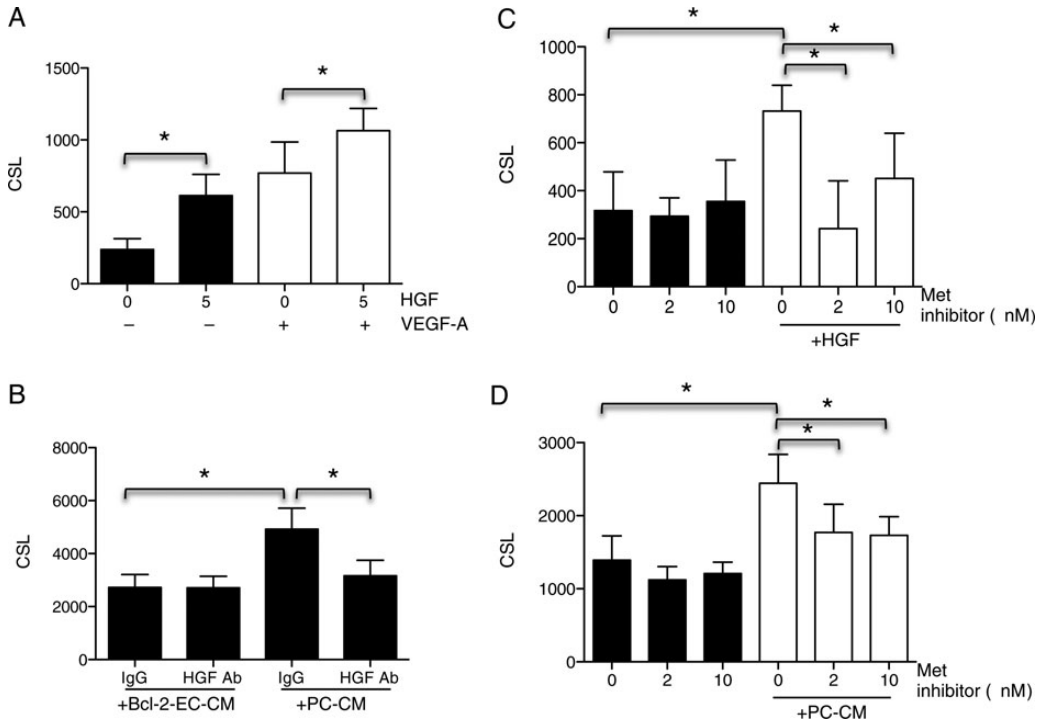

Figure 3 PC-secreted HGF stimulates Bcl-2-EC sprouting. (*A*) Basal Bcl-2-EC CSL and responses to recombinant HGF (5 ng/mL) without or with VEGF-A (100 ng/mL). (*B*) One of three independent experiments depicting Bcl-2-EC CSL in the presence of Bcl-2-EC-CM or PC-CM immunodepleted with control IgG or anti-HGF antibody. (*C* and *D*) Bcl-2-EC CSL without or with 5 ng/mL HGF or PC-CM and 0, 2, or 10 nM of c-Met receptor tyrosine kinase (Met) inhibitor. The asterisk indicates a statistically significant difference by a two-tailed *t*-test with *post hoc* Bonferroni corrections ($P < 0.025$ for *A*, $P < 0.025$ for both comparisons in *B*, and $P < 0.017$ for *C* and *D*).

PDGFR-β was critical for PC recruitment by Bcl-2-EC sprouts, we knocked down PDGFR-β in PCs by siRNA (*Figure 5A*). Bcl-2-EC and PC association was decreased and Bcl-2-EC sprouting was increased (*Figure 5B–D*). Cumulatively, these data suggest that PDGFR-β signalling promotes recruitment of PCs to the sprouts formed from Bcl-2-EC/PC mixed spheroids and that contact between Bcl-2-ECs and PCs inhibits the PC stimulatory effect. We observed no difference in PDGF-B expression when we compared Bcl-2-EC vs. non-transduced EC (see Supplementary material online, *Figure S3*) suggesting that recruitment was not mediated by Bcl-2 effects on PDGF-B expression.

Since isolated PCs stimulate EC sprouting by release of HGF and since PCs in contact with EC sprouts halt increases in CSL, we investigated if contact with Bcl-2-ECs could affect the expression of HGF in PCs. To do so, we compared HGF mRNA levels of PCs in mixed spheroids, where contact with ECs occurs, vs. mRNA levels in PC-only spheroids, i.e. in the absence of contact with ECs. Consistent with an inhibitory effect of EC contact, we found that PCs expressed significantly less HGF when in contact with Bcl-2-ECs in mixed spheroids compared with that in PC-only spheroids (see Supplementary material online, *Figure S4*). Cell contact appeared necessary for this inhibitory effect as EC-CM or ECs across a transwell actually stimulated PC production of HGF (W.G.C., unpublished data).

3.3 Microvascular formation from *in vivo* implantation of EC and mixed spheroids

It had been reported that HUVEC spheroids implanted into immunodeficient mice within protein gels form sprouts that anastomose with host microvessels, giving rise to human EC-lined microvessels.[24] To assess the effects of PCs on vessel formation from EC spheroids *in vivo*, we compared microvessel formation by EC and EC-PC spheroids within collagen gels after implantation into immunodeficient mice. Here, we use non-transduced ECs, because Bcl-2 transduction is not required for EC survival in collagen gel implants *in vivo*.[11] Previous studies showed that single cell suspensions containing PCs or SMCs resulted in contraction of collagen/fibronectin gels and concomitant loss of cell viability that could be prevented by forming gels within poly(glycolic acid) (PGA) scaffolds.[16,18] In contrast, we did not observe contraction of gels when PCs were introduced into gels as components of mixed spheroids. This allowed us to examine implantation of gels containing mixed spheroids in immunodeficient mice without PGA scaffolds. Gels were harvested 4 weeks after implantation for immunohistochemistry/immunofluorescence, vessel density, and morphology. Implantation of EC and EC-PC mixed spheroids each resulted in human EC-lined channels containing mouse erythrocytes, indicative of perfusion (*Figure 6A*). No statistically significant difference in vessel density was observed by a two-tailed *t*-test (*Figure 6B*). However, luminal diameters were significantly smaller in EC-PC-derived vessels when compared with those from EC-only spheroids (*Figure 6C*). TEM using iron-labelled PCs confirmed close contact of ECs and PCs in microvessels formed *in vivo* (*Figure 6D*).

The microvessels that formed from EC and EC-PC spheroids were lined by human ECs assessed by human-specific Ulex Europaeus Agglutinin-I (UEA-1) staining and surrounded by mural cells expressing SMA (*Figure 6E* and *H*). The anti-SMA antibody used cannot distinguish between mouse and human versions of this protein. To determine the

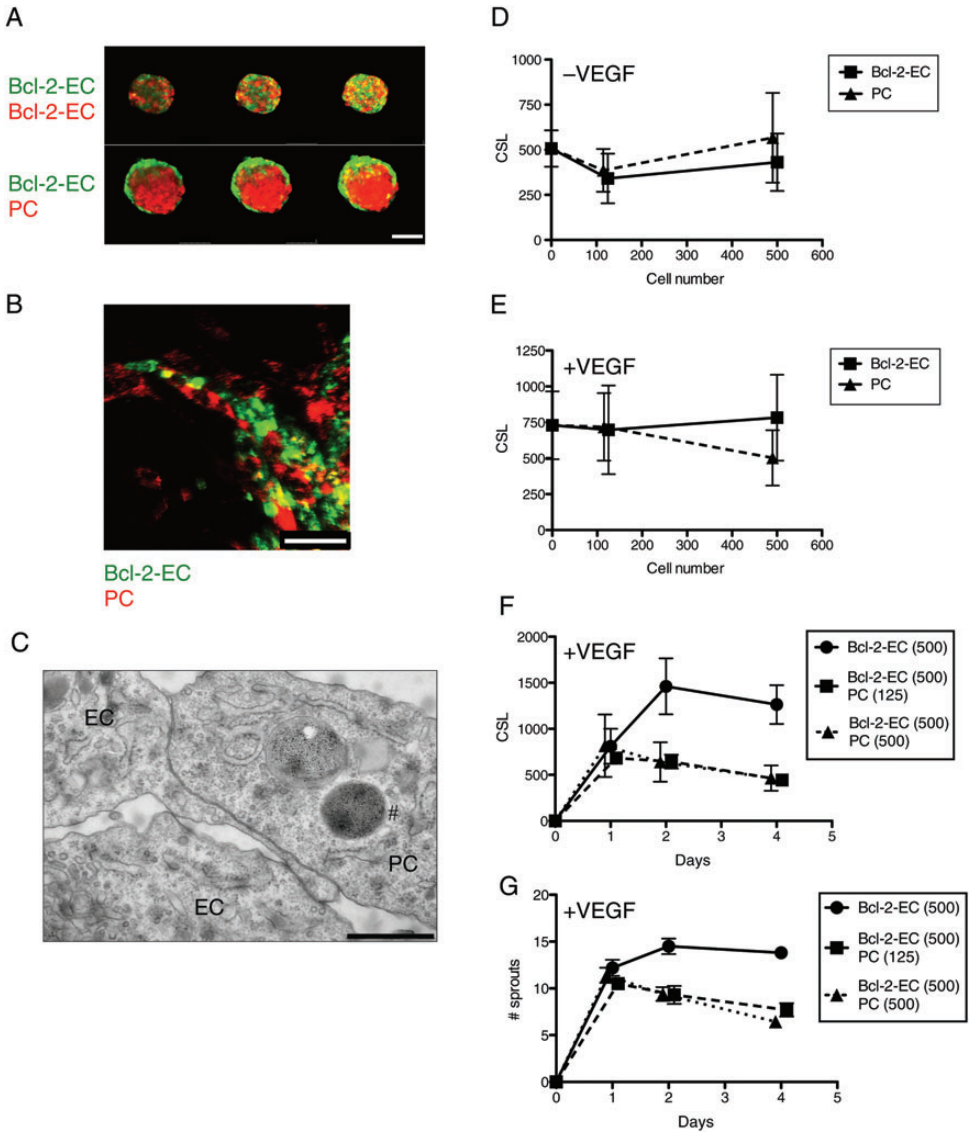

Figure 4 Sprout formation by mixed spheroids. (*A*) Organization of Bcl-2-ECs and PCs in mixed spheroids. Mixed spheroids of 500 Bcl-2-ECs (PKH67 green-labelled cells) + 125 Bcl-2-ECs (PKH26 red-labelled cells) and 500 Bcl-2-ECs (green) + 125 PCs (red) were formed, transferred to collagen gels, and immediately imaged by confocal *Z*-series. Serial slices with 10 μm step size are shown. The scale bar is 75 μm. (*B*) Confocal fluorescence images of 500 Bcl-2-ECs (PKH67 green-labelled cells) with 125 PCs (PKH26 red-labelled cells) in mixed spheroid collagen gels with 100 ng/mL VEGF-A. The scale bar is 75 μm. (*C*) TEM showing association of a PC with a Bcl-2-EC sprout within an *in vitro* gel after 3 days. #An endosome within the PC-containing iron nanoparticles used to pre-label the PCs. The scale bar is 1 μm. (*D* and *E*) CSL ± SD of Bcl-2-EC sprouts in the presence of increasing numbers of Bcl-2-ECs and PCs in mixed spheroids without (*C*) or with (*D*) 100 ng/mL VEGF-A after 24 h. (*F* and *G*) CSL and sprout number over a 4-day time course. Bcl-2-EC spheroids containing 500 cells per spheroid were compared with mixed spheroids containing an additional 125 or 500 PCs.

origin of these mural cells, sections were co-stained with W6/32, a marker of human leukocyte antigen (HLA), and anti-SMA (*Figure 6F* and *I*). No HLA/SMA co-localization was seen in microvessels formed by EC-only spheroids (*Figure 6F*), arguing against a human origin for these SMA-positive cells. Instead, it appeared that mural cells were derived from the mouse host, as we saw co-localization of SMA with mouse H-2K^d within the gels (*Figure 6G*). In contrast, we observed HLA/SMA double positive cells when vessels were derived from EC-PC mixed spheroids (*Figure 6I*). We did not see co-localization of SMA and H-2K^d in vessels derived from EC-PC mixed spheroids (*Figure 6J*), arguing that most mural cells were derived from the implanted human PCs.

4. Discussion

Here, we have described both paracrine and contact permissive *in vitro* spheroid models to study how PCs affect EC sprouting. We have expanded the capacity to study ECs in 3D culture over time by transducing cells with Bcl-2. We observed three differences between HUVECs transduced with Bcl-2 vs. non-transduced ECs, namely that Bcl-2-ECs implanted as spheroids can survive in collagen gels *in vitro* for extended periods, allowing sprouting to be observed over days; that Bcl-2-ECs spontaneously sprout to a limited extent in a manner independent of VEGF; and that Bcl-2-ECs are more sensitive to the effects of VEGF,

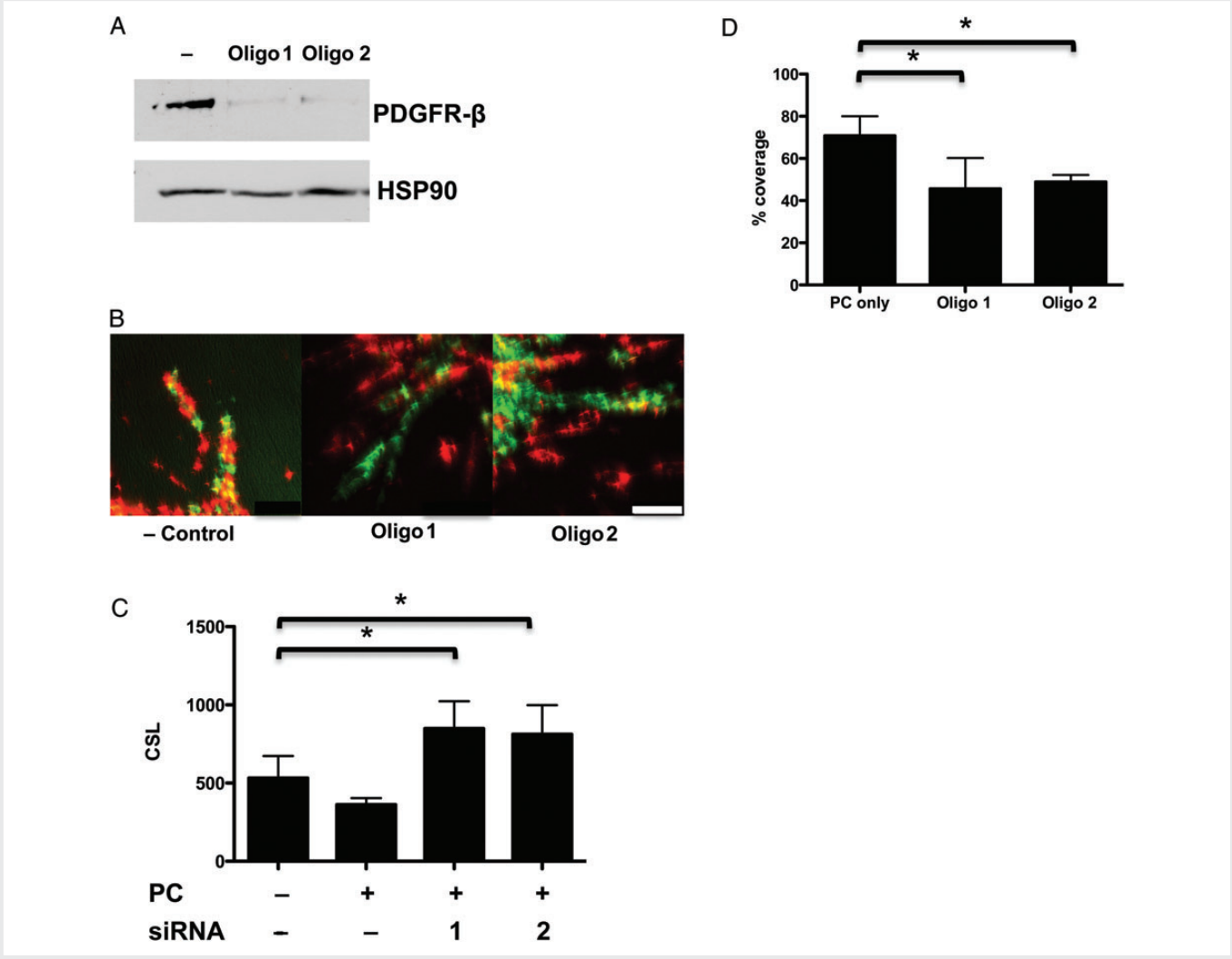

Figure 5 Bcl-2-EC sprouts restrained by PDGFR-β-mediated interactions. PCs treated with negative control, PDGFR-β siRNA oligo 1, or 2. (*A*) Immunoblot of PC protein extracts detected with anti-PDGFR-β and HSP-90 as the loading control. (*B*) Confocal fluorescence images of mixed spheroids with 500 Bcl-2-ECs (PKH67 green-labelled cells) + 125 PCs (PKH26 red-labelled cells) treated with 100 ng/mL VEGF-A. The scale bar is 50 μm. (*C*) CSL and (*D*) percentage of Bcl-2-EC sprouts covered by PCs after PDGFR-β knockdown. The asterisk indicates a statistically significant difference by a two-tailed *t*-test with *post hoc* Bonferroni correction ($P < 0.025$ for *D*).

responding to lower concentrations of growth factor. Nevertheless, both EC types respond to VEGF by forming sprouts. We are currently exploring the mechanisms behind VEGF-independent basal Bcl-2-EC sprouting. We found that PCs secrete significant quantities of HGF that can be a potent paracrine angiogenic stimulus for EC sprouting, acting in concert with VEGF on either control or Bcl-2-ECs, and that PCs can restrain sprouting under conditions that permit EC-PC contact, i.e. during sprouting from mixed spheroids *in vitro*. The latter effect can only be studied using Bcl-2-ECs as sprout survival is necessary for efficient investment and this system allowed us to demonstrate that investment of EC sprouts by PCs in this model is dependent upon PDGFR-β, similar to what has been observed both *in vivo*[18–20] and using suspended cells *in vitro*.[25]

HGF, also known as 'scatter factor', binds to the c-Met receptor tyrosine kinase to regulate developmental morphogenesis, tissue remodelling, regeneration, wound repair, and tumour invasion.[26] ECs express the c-Met receptor, and HGF has been shown to stimulate EC invasion into 3D collagen gels and to stimulate vessel growth *in vivo* in a rabbit cornea angiogenesis model.[20] Recent data have demonstrated that both fibroblasts and SMCs also secrete HGF to stimulate EC sprouting from spheroids formed on beads.[27] Given the presence of PCs in the walls of microvessels from which sprouts originate, the observation that PCs express such significant amounts of HGF implies that PCs may play a critical role in supporting sprout formation.

In addition to the paracrine signalling models described, we used mixed-cell spheroids to examine cell contact-dependent interactions. When we formed mixed spheroids using ECs and PCs, we observed that PCs initially localized to the core of the spheroid. This behaviour was previously reported with EC/SMC mixed spheroids.[11] The biological significance of this is unclear since spheroids lack lumens and thus the abluminal and luminal sides are not clearly defined. Bcl-2-EC/PC mixed spheroids in our system did not show an increase in EC sprouting compared with pure EC spheroids within 24 h; however, PCs limited sprout number and sprout lengths by Day 2. Time-lapse videography indicates

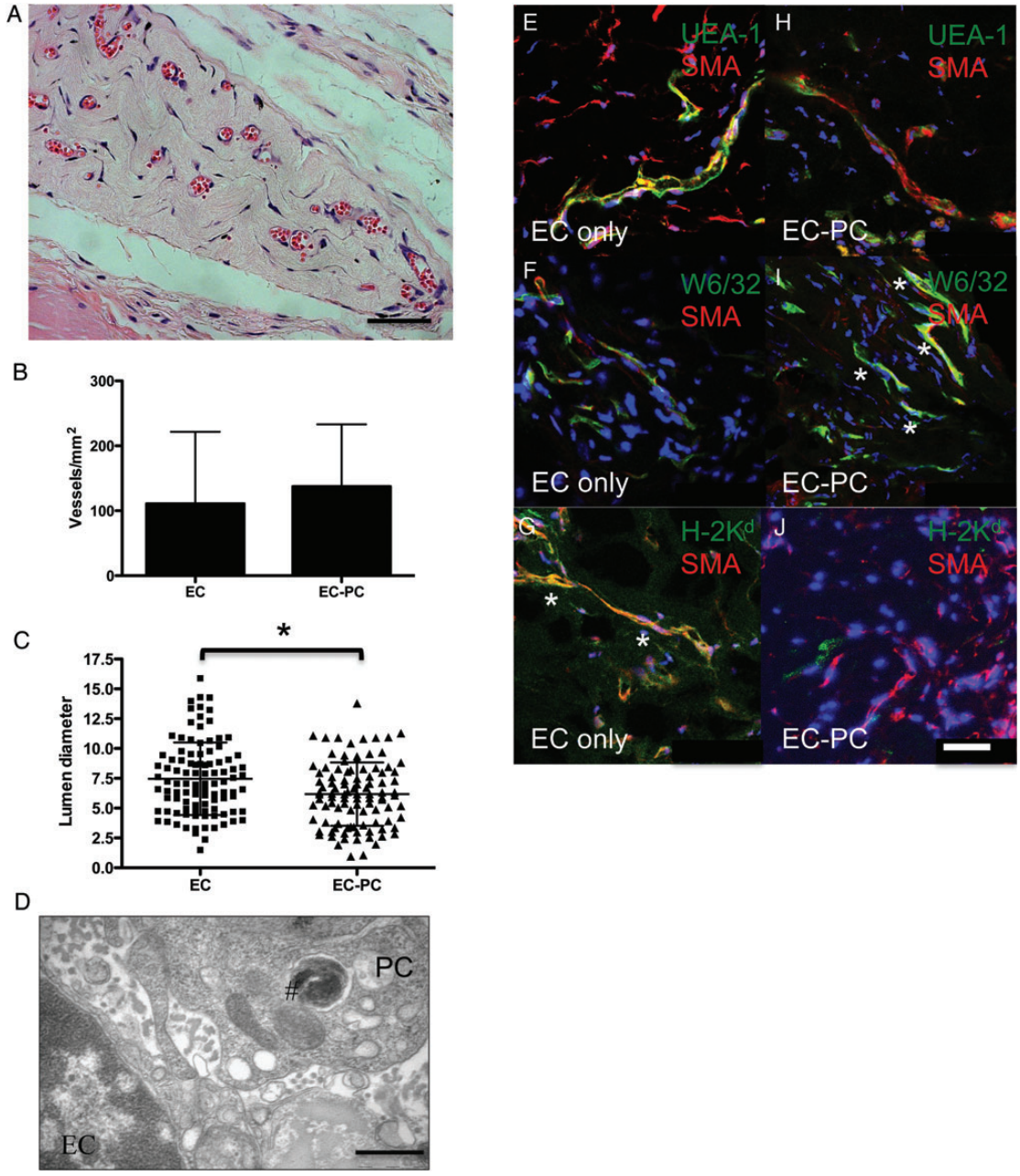

Figure 6 Microvessel formation from EC and EC-PC mixed spheroids *in vivo*. (*A*) Representative H&E staining of collagen gel implant from EC-PC mixed spheroids showing RBC perfusion. The scale bar is 50 μm. (*B*) Microvessel density ± SD from EC and EC-PC groups. (*C*) The scatter plot with mean ± SD of vessel diameters. The asterisk indicates a statistically significant difference between groups by a two-tailed *t*-test, $P = 0.0015$. (*D*) TEM of EC and PC interaction in a microvessel. #Iron-labelled endosome in PC. The scale bar is 1 μm. (*E–J*) Merged confocal images of fluorescence staining of vessels from (*E–G*) EC only and (*H–J*) EC-PC spheroids from frozen sections. (*E* and *H*) Human ECs stain with fluorescein isothiocyanate UEA-I (green) and mural cells with SMA (red). (*F* and *I*) Cells expressing human class I major histocompatibility complex (MHC) molecules (HLA-A, B) stain with mAb W6/32 (green). In vessels from (*F*) EC-only spheroids, W6/32 (green) and SMA (red) do not, but in (*I*) EC-PC spheroids W6/32 and SMA do co-localize. (*G* and *J*) Cells expressing mouse class I MHC molecules stain with H-2K^d (green). In vessels from (*G*) EC-only spheroids, H-2K^d (green) and SMA (red) do co-localize, but in (*J*) EC-PC spheroids do not. The asterisk highlights areas of co-localization. Hoechst staining in blue. The scale bar is 50 μm.

that this delay in the limiting effect of PCs is likely due to the fact that Bcl-2-ECs initially sprout independently of PCs, and only later, between 9 and 19 h, recruit PCs that migrate outwards from the spheroids. Using confocal fluorescence microscopy, we saw that siRNA knockdown of PDGFR-β reduced PC coverage of Bcl-2-EC sprouts and enhanced Bcl-2-EC sprouting. This is consistent with the known role of PDGFR-β in the recruitment of PCs to microvessels. In addition, we observe that PCs in contact with ECs in the mixed spheroids down-regulate HGF gene expression. An EC contact-dependent reduction in PC elaboration of HGF is consistent with the observation that PCs in contact with Bcl-2-ECs do not have a net stimulatory effect on Bcl-2-EC sprouting in the mixed spheroids.

A mixed spheroid model was previously used to examine interactions of ECs and arterial SMCs.[11] While interactions between these cell types are important in larger vessels, the principal mural cells in microvessels that give rise to sprouts are PCs. We have seen significant differences between human placental PCs and human umbilical artery SMCs that clearly distinguish these cell types. Specifically, in the mixed spheroid model *in vitro*, we observed that SMCs do not efficiently invest EC sprouts but instead significantly stimulate EC sprouting rather than contain it (see Supplementary material online, *Figure S2*). The EC spheroid model results in sprouts that only minimally lumenize *in vitro*, a limitation of this model for the study of this aspect of angiogenesis. However, EC spheroids do give rise to lumenized EC-lined microvessels *in vivo*. Furthermore, following implantation *in vivo*, the presence of SMCs in mixed spheroids actually increases the resultant luminal diameters compared with EC-only spheroids (W.G.C., unpublished data) in contrast to the effects of PCs to reduce lumen size (*Figure 6C*). Similar differences *in vivo* between vessels formed by ECs in the presence of PCs vs. SMCs using cells individually suspended within PGA-supported collagen gels were observed previously.[13,15] The capacity of PCs to limit the luminal diameter of EC tubes formed *in vitro* has recently been reported by others using human brain PCs[25] and by us using placental microvascular PCs.[28] While these findings suggest intrinsic differences between PCs and SMCs, we caution that we have to date only tested HUVECs, placental PCs, and umbilical artery or aortic SMCs as model cell types. It is possible that vascular cells derived from other origins may have different characteristics.

The studies reported here not only have implications for understanding sprouting in angiogenesis, but also may be useful for tissue engineering. We observed that EC-only and EC-PC mixed spheroids could each generate human EC-lined microvessels and that the microvessels that formed were invested by mural cells that expressed SMA. This differs from our previous observation that non-transduced ECs failed to recruit mural cells when freely suspended within collagen/fibronectin gels and implanted,[13] and represents an unanticipated advantage of engineering microvessels with spheroids. Implantation of mixed spheroids instead of individually suspended cells also allows for the introduction of contractile mural cells without the need for a PGA-scaffold to prevent gel contraction. This simple technique, which has not been previously described, may be a solution to the general problem of using contractile cells in protein gels for tissue engineering. Future studies with cells from other sources may lead to the construction of microvessels specialized for particular tissues and may be applied to improve the outcomes of cell transplant therapy or tissue engineering.

Supplementary material

Supplementary material is available at *Cardiovascular Research* online.

Acknowledgements

VEGF-A was obtained from the NCI BRB Preclinical Repository. We thank the Yale Center for Analytical Science for discussion of statistical analysis and Morven Graham (Yale University, New Haven, CT, USA) for assistance with EM.

Conflict of interest: none declared.

Funding

This work was supported by National Institutes of Health Grants (R01-HL085416 to J.S.P and W.M.S.), (T32-DK007276 to W.G.C.), and a Clinical and Translational Science Award (KL2-RR024138 to W.G.C.) from the National Center for Advancing Translational Science. Its contents are solely the responsibility of the authors and do not necessarily represent the official view of NIH.

References

1. Simons M. Angiogenesis: where do we stand now?. *Circulation* 2005;**111**:1556–1566.
2. Adams RH, Alitalo K. Molecular regulation of angiogenesis and lymphangiogenesis. *Nat Rev Mol Cell Biol* 2007;**8**:464–478.
3. Lieu C, Heymach J, Overman M, Tran H, Kopetz S. Beyond VEGF: inhibition of the fibroblast growth factor pathway and antiangiogenesis. *Clin Cancer Res* 2011;**17**:6130–6139.
4. Potente M, Gerhardt H, Carmeliet P. Basic and therapeutic aspects of angiogenesis. *Cell* 2011;**146**:873–887.
5. Ribatti D, Nico B, Crivellato E. The role of pericytes in angiogenesis. *Int J Dev Biol* 2011;**55**:261–268.
6. Hellström M, Gerhardt H, Kalén M, Li X, Eriksson U, Wolburg H *et al*. Lack of pericytes leads to endothelial hyperplasia and abnormal vascular morphogenesis. *J Cell Biol* 2001;**153**:543–553.
7. Hammes HP, Lin J, Wagner P, Feng Y, Vom Hagen F, Krzizok T *et al*. Angiopoietin-2 causes pericyte dropout in the normal retina: evidence for involvement in diabetic retinopathy. *Diabetes* 2004;**53**:1104–1110.
8. Morikawa S, Baluk P, Kaidoh T, Haskell A, Jain RK, McDonald DM. Abnormalities in pericytes on blood vessels and endothelial sprouts in tumors. *Am J Pathol* 2002;**160**:985–1000.
9. Goodwin AM. In vitro assays of angiogenesis for assessment of angiogenic and anti-angiogenic agents. *Microvasc Res* 2007;**74**:172–183.
10. Korff T, Augustin H. Integration of endothelial cells in multicellular spheroids prevents apoptosis and induces differentiation. *J Cell Biol* 1998;**143**:1341–1352.
11. Korff T, Kimmina S, Martiny-Baron G, Augustin HG. Blood vessel maturation in a 3-dimensional spheroidal coculture model: direct contact with smooth muscle cells regulates endothelial cell quiescence and abrogates VEGF responsiveness. *FASEB J* 2001;**15**:447–457.
12. Ilan N, Mahooti S, Madri JA. Distinct signal transduction pathways are utilized during the tube formation and survival phases of in vitro angiogenesis. *J Cell Sci* 1998;**111**(Pt 24):3621–3631.
13. Schechner J, Nath A, Zheng L, Kluger M, Hughes C, Sierra-Honigmann M *et al*. In vivo formation of complex microvessels lined by human endothelial cells in an immunodeficient mouse. *Proc Natl Acad Sci USA* 2000;**97**:9191–9196.
14. Enis D, Shepherd B, Wang Y, Qasim A, Shanahan C, Weissberg P *et al*. Induction, differentiation, and remodeling of blood vessels after transplantation of Bcl-2-transduced endothelial cells. *Proc Natl Acad Sci USA* 2005;**102**:425–430.
15. Zheng L, Ben LH, Pober JS, Bothwell AL. Porcine endothelial cells, unlike human endothelial cells, can be killed by human CTL via Fas ligand and cannot be protected by Bcl-2. *J Immunol* 2002;**169**:6850–6855.
16. Maier C, Shepherd B, Yi T, Pober J. Explant outgrowth, propagation and characterization of human pericytes. *Microcirculation* 2010;**17**:367–380.
17. Gimbrone MA. Culture of vascular endothelium. *Prog Hemost Thromb* 1976;**3**:1–28.
18. Shepherd BR, Jay SM, Saltzman WM, Tellides G, Pober JS. Human aortic smooth muscle cells promote arteriole formation by coengrafted endothelial cells. *Tissue Eng Part A* 2009;**15**:165–173.
19. Grant DS, Kleinman HK, Goldberg ID, Bhargava MM, Nickoloff BJ, Kinsella JL *et al*. Scatter factor induces blood vessel formation in vivo. *Proc Natl Acad Sci USA* 1993;**90**:1937–1941.
20. Bussolino F, Di Renzo MF, Ziche M, Bocchietto E, Olivero M, Naldini L *et al*. Hepatocyte growth factor is a potent angiogenic factor which stimulates endothelial cell motility and growth. *J Cell Biol* 1992;**119**:629–641.
21. Levéen P, Pekny M, Gebre-Medhin S, Swolin B, Larsson E, Betsholtz C. Mice deficient for PDGF B show renal, cardiovascular, and hematological abnormalities. *Genes Dev* 1994;**8**:1875–1887.
22. Soriano P. Abnormal kidney development and hematological disorders in PDGF beta-receptor mutant mice. *Genes Dev* 1994;**8**:1888–1896.
23. Lindahl P, Johansson BR, Levéen P, Betsholtz C. Pericyte loss and microaneurysm formation in PDGF-B-deficient mice. *Science* 1997;**277**:242–245.
24. Alajati A, Laib AM, Weber H, Boos AM, Bartol A, Ikenberg K *et al*. Spheroid-based engineering of a human vasculature in mice. *Nat Methods* 2008;**5**:439–445.
25. Stratman AN, Schwindt AE, Malotte KM, Davis GE. Endothelial-derived PDGF-BB and HB-EGF coordinately regulate pericyte recruitment during vasculogenic tube assembly and stabilization. *Blood* 2010;**116**:4720–4730.
26. Trusolino L, Bertotti A, Comoglio PM. MET Signalling: principles and functions in development, organ regeneration and cancer. *Nat Rev Mol Cell Biol* 2010;**11**:834–848.
27. Newman AC, Chou W, Welch-Reardon KM, Fong AH, Popson SA, Phan DT *et al*. Analysis of stromal cell secretomes reveals a critical role for stromal cell-derived hepatocyte growth factor and fibronectin in angiogenesis. *Arterioscler Thromb Vasc Biol* 2013;**33**:513–522.
28. Waters JP, Kluger MS, Graham M, Chang WG, Pober JS. In vitro self-assembly of human pericyte-supported endothelial microvessels in three-dimensional co-culture: a simple model for interrogating endothelial-pericyte interactions. *J Vasc Res* 2013;**50**:324–331.